Angular Distributions and Correlations for Alpha-Particle Scattering by C^{12}, Mg^{24}, and Ca^{40}*

G. B. SHOOK†
University of Washington, Seattle, Washington
(Received November 14, 1958)

Angular distributions of alpha particles scattered from Mg^{24} and Ca^{40} are reported and effective interaction radii are obtained, based on the Born approximation for elastic scattering and direct-interaction theory for inelastic scattering. For Mg^{24}, levels at 0, 1.37, 4.2, and 6.3 Mev yield interaction radii of 6.4, 6.55, 6.5, and 6.5, respectively (units of 10^{-13} cm). Evidence is presented in support of the assignment of the 6.3-Mev level to Mg^{24} rather than to Mg^{25} or Mg^{26}, with spin and parity $1-$. For Ca^{40}, levels at 0 and 4.48 Mev yield interaction radii of 6.65 and 7.3, respectively. Alpha-gamma angular correlations, which correspond closely to those predicted on the basis of direct-interaction theory, were obtained for C^{12} (4.43-Mev level) and for Mg^{24} (1.37-Mev level). For Ca^{40} (4.48-Mev level) the correlation corresponds qualitatively to that predicted for a $1-$ level with cascade decay through an intermediate state to ground level. Further evidence is presented which supports this interpretation. A higher level in Ca^{40} is observed at 8.4 Mev. All alpha bombardments were made at 43 Mev incident energy.

I. INTRODUCTION

SINCE the advent of direct-interaction theory[1,2] to explain the behavior of scattering of nucleons by nuclei, several angular distributions of scattering processes have been compared with the theoretical predictions.[3–14] These comparisons, in general, seem to indicate indifferent fits of data to the theory in the cases of proton scattering, and fair to good fits for alpha scattering. With regard to the theoretical treatment of the interaction, the comparisons almost invariably involve several simplifying assumptions, among which are (a) surface interaction, (b) elementary nucleon-nucleon interaction independent of angle and energy, and (c) plane waves for bombarding and scattered nucleons at the nuclear surface.

Since the possibility exists that at least a portion of the observed scattering might be due to compound nuclear interaction, Satchler[15] suggested that angular correlations between scattered particles and subsequent gamma radiation from the excited target nuclei might provide a definite means of distinguishing between direct and compound nuclear interaction.

Banerjee and Levinson[16] analyzed the effect of the assumption of plane waves *versus* distorted waves for the incident and scattered nucleons on the cross section. They were able to show that, in a direct interaction, the formula of the correlation is essentially unchanged from that predicted by plane waves, but that distorted waves lead, in general, to a shift in the symmetry axis for the correlation. They also pointed out that to be consistent, the same wave forms which best explain the angular distribution should give the correct shift of the correlation symmetry axis. Their application of these principles to the data of Hornyak and Sherr[12,16] resulted in a convincing demonstration of the validity of the direct-interaction model when distorted waves are used.

A primary purpose of the present work was to extend the experimental data to cases not yet considered, in order to provide a wider comparison of theory and experiment. The work consisted of obtaining angular correlations between inelastically scattered alpha particles and the resultant gamma rays together with the angular distributions of the scattered alpha particles for three target nuclei (C^{12}, Mg^{24}, Ca^{40}) and to compare their relative deviations from the plane wave predictions.

II. EXPERIMENTAL

A. General

The data reported here were obtained in the 24-in. scattering chambers which at present represents the end of the line for the external beam of the University of Washington cyclotron.

Angular distributions were obtained with a thin NaI(Tl) crystal scintillator mounted on a 6291 photo-

* This work was supported in part by the U. S. Atomic Energy Commission.

† Now at Lockheed Aircraft Corporation, Missile Systems Division, Palo Alto, California.

[1] G. F. Chew, Phys. Rev. **80**, 196 (1950).
[2] Austern, Butler, and McManus, Phys. Rev. **92**, 350 (1953).
[3] H. J. Watters, Phys. Rev. **103**, 1763 (1956).
[4] P. C. Gugelot and M. Rickey, Phys. Rev. **101**, 1613(L) (1956).
[5] F. J. Vaughn, University of California Radiation Laboratory Report UCRL-3174, 1955 (unpublished).
[6] Seidlitz, Bleuler, and Tendom, Bull. Am. Phys. Soc. Ser. II, **1**, 29 (1956).
[7] R. G. Summers-Gill, University of California Radiation Laboratory Report UCRL-3388, 1956 (unpublished).
[8] R. G. Summers-Gill, Phys. Rev. **109**, 1591 (1958).
[9] G. W. Farwell and D. D. Kerlee, Bull. Am. Phys. Soc. Ser. II, **1**, 20 (1956).
[10] R. W. Peele, Phys. Rev. **105**, 1311 (1957).
[11] H. E. Conzett, Phys. Rev. **105**, 1324 (1957).
[12] R. Sherr and W. F. Hornyak, Bull. Am. Phys. Soc. Ser. II, **1**, 197 (1956).
[13] P. C. Robison, Ph.D. thesis, University of Washington (unpublished).
[14] A. Yavin, Ph.D. thesis, University of Washington (unpublished).
[15] G. R. Satchler, Proc. Phys. Soc. (London) **A68**, 1037 (1955).
[16] M. K. Banerjee and C. A. Levinson, Ann. Phys. **2**, 499 (1957); C. A. Levinson and M. K. Banerjee, Ann. Phys. **3**, 67 (1958).

multiplier tube. Normalization of the alpha-particle beam was achieved by means of integration of charge collected in a Faraday cup, and by monitoring of scattered particles with an auxiliary counter mounted at a fixed angle with respect to the beam.

Angular correlations were obtained by the use of the thin NaI alpha-particle detector at a fixed angle, together with a variable-angle gamma-ray detector consisting of a $1\frac{3}{4}\times 2$-in. NaI(Tl) crystal mounted on a 6292 photomultiplier tube, with crystal and tube almost completely surrounded by a heavy lead shield. The gamma-ray detector was moved through approximately one quadrant coplanar with incident beam and particle detector in obtaining the correlation.

Signals from particle detector and gamma-ray detector were compared in a fast coincidence circuit for detection of simultaneous events.

All alpha bombardment runs were made at 43-Mev incident energy. A few proton bombardment runs were made (see Sec. IV C) at an incident energy of 11 Mev.

The external beam system and scattering chamber are described elsewhere[13] and will not be dwelt upon here except as noted in the following paragraphs.

B. Target Materials

The carbon target for the $C^{12}(\alpha,\alpha'\gamma)$ angular correlation study consisted of a small disk of 4-mil polyethylene. No difficulty was encountered in resolving the 4.43-Mev energy level in C^{12} with this comparatively thick (10 mg/cm^2) target.

Natural magnesium foil, 1.1 mg/cm^2, was used for the $Mg^{24}(\alpha,\alpha')$ angular distribution measurements. Six thicknesses of this foil were used for the $Mg^{24}(\alpha,\alpha'\gamma)$ angular correlation study; even so, the 1.37-Mev level in Mg^{24} was resolved nearly as well as when the single thickness was used.

Natural calcium foil was made by vacuum evaporation of calcium turnings from a tungsten boat onto a Pyrex plate, whence a foil was stripped and a section chosed as a target having a thickness of 13.4 mg/cm^2 for the $Ca^{40}(\alpha,\alpha'\gamma)$ angular correlation study; another section of 6 mg/cm^2 was used for the $Ca^{40}(\alpha,\alpha')$ angular distribution measurements. A first attempt at this technique resulted in a badly oxidized foil; in the second trial, the evaporator was filled with argon after the foil deposition, and subsequent handling of the foil was always done in an argon atmosphere. This proved satisfactory, with only minor impurities showing up in the angular distribution.

C. Electronics and Gamma-Ray Shielding

The use of 43-Mev alpha particles gave rise to a large background of gamma radiation, especially from collimators which defined a $\frac{1}{8}$-in. diam beam incident on the target. In addition to the 2 in. of lead surrounding the gamma detector, approximately 6 in. of lead shielding was placed about the collimator, with lesser amounts of shielding at other points. Even so, a number of measures were required to obtain resolvable gamma spectra from the target. Among these measures were relatively thick targets combined with a large acceptance angle (a cone of 21° 20′ half-angle) for the gamma detector, low beam intensity (10^{-9} ampere or less) incident on the target, and fast coincidence techniques. (Time resolution 0.025 μsec.) In the coincidence work, a 40-channel analyzer was used to obtain first an ungated alpha-particle spectrum, then a gated spectrum for each angle setting of the detectors. The comparison of the spectra corresponding to elastically scattered alphas then gave the chance to true coincidence ratio. This method proved as reliable as the more usual technique of introducing a time delay in one branch of the fast coincidence circuit and saved an appreciable amount of cyclotron running time.

In a few runs, protons were used in place of alphas as bombarding particles for purposes of calibration or, in the case of calcium, to investigate the decay mode of the 4.48-Mev level. Here the gamma background was very substantially reduced due to the lower (11 Mev) energy of protons from the cyclotron.

III. THEORY

A. Angular Correlation

The general theory of angular correlation is well developed, with several comprehensive and rigorous treatments of the subject now in the literature.[17] The application of this theory to direct interaction processes[15,16] leads to the unambiguous prediction that the gamma distribution, taken in coincidence with the emergent nucleons, will have a form characteristic of the multipolarity of the nuclear de-excitation transition, with a certain symmetry axis θ_0 for the simple cases of single, pure transitions. With the simplifying assumptions of surface interaction, plane waves, and zero-range forces, θ_0 is just the recoil direction θ_R of the target nucleus. Thus, any deviation of θ_0 from θ_R is a measure of the deviation of the nature of the actual process from these assumptions, and a failure to observe the multipole pattern would constitute a challenge to the validity of the direct-interaction theory for the case under study.

As pointed out by Satchler,[15] the prediction of symmetry of the multipole pattern about θ_0 is in sharp contrast with the predictions of compound-nucleus theory where the recoil axis has no special significance with regard to the distribution of gammas.

For the specific cases of $X(\alpha,\alpha')X^*(\gamma)X$, where X is an even-even nucleus, with ground state spin and parity 0+, the correlation is given specifically by Biedenharn and Rose [reference 17, p. 752, Eq. (80)]

[17] E.g., L. C. Biedenharn and M. E. Rose, Revs. Modern Phys. 25, 729 (1953); G. Racah, Phys. Rev. 84, 910 (1951).

to be

$$W(\theta)=\sum A_\nu \frac{2l(l+1)}{2l(l+1)-\nu(\nu+1)} P_\nu(\cos\theta),$$

where

$$A_\nu=F_\nu(L_1 j_1 j)F_\nu(L_2 j_2 j),$$

and ν is a summation index which is restricted by vector addition rules and parity considerations to be integral and even, with $\nu_{\max}$ equal to or less than the smallest of $2j_1$, $2L_1$, $2L_2$. The j_1, j, and j_2 are nuclear spins for initial, intermediate, and final states, respectively, of the target nucleus, while L_1 and L_2 are the changes in orbital angular momenta occurring in the transitions $j_1 \rightarrow j$ and $j \rightarrow j_2$, respectively. The $P_\nu(\cos\theta)$ are Legendre polynomials, with θ the angle between the observed alpha and gamma, or, equivalently, between the recoil direction and the gamma. The effect of this interchange of angles on the solid angle correction is discussed further in Sec. V. The l is understood to replace L_1 or L_2 in the F functions according as to whether the alpha particle is emitted in the $j_1 \rightarrow j$ or $j \rightarrow j_2$ transition, and for the experiments reported herein, is always the former. The F functions are tabulated in reference 17, pp. 746–748.

B. Angular Distributions

At least three types of direct-interaction theories have been presented in attempts to provide an explanation of the diffraction-like scattering pattern so frequently observed. Austern, Butler, and McManus,[2] hereafter abbreviated as ABM, have developed a theory involving interaction of the bombarding particle with elementary nucleons near the nuclear surface. This theory is usually developed so as to separate the cross section magnitude from the angular dependence, where the magnitude involves a calculation of the radial wave function and elementary cross section for scattering between the incident particle and a nucleon near the nuclear surface, while the angular dependence is contained in spherical Bessel functions $j_l(Kr)$. Here, l is the order of the Bessel function, $\hbar K$ is the momentum transferred from incident particle to nucleus, and r is the interaction radius at which the transfer takes place. Blair and Henley[18] suggest that the elementary interaction might take place between incident particle and groups of nucleons (such as alpha particles) in the target nucleus. The angular dependence again is contained in the spherical Bessel functions. Hayakawa and Yoshida[19] extend the concept of the elementary interaction still farther to be between the incoming particle and collective modes of motion of the target nucleus, where the collective modes are assumed to be those described by Bohr and Mottelson.[20] Spherical Bessel functions again describe the angular dependence of the scattering. In all three cases, the angular dependence in terms of simple functions is a consequence of certain simplifying assumptions. These assumptions are (a) interaction at the nuclear surface, (b) no angular or energy dependence is involved in the elementary interaction, and (c) the bombarding and scattered nucleons can be described by plane waves in the region of the nuclear surface.

Using direct-interaction theory together with the simplifying assumptions previously listed of plane waves, delta-function interaction, and evaluation of the $j_l(Kr)$ at the nuclear surface $r=R$ [hereafter, the abbreviation $j_l(KR)=j_l(\rho)$ will be used], one obtains two kinds of information from a comparison of theory with experiment: values of the effective interaction radius R and the values of l pertinent to a particular transition being investigated. As long as the simplifying assumptions are retained, this is nearly all that can be hoped for, although an absolute magnitude experiment could also yield cross-section measurements which could be then compared with the predictions of the various types of direct-interaction theory for differential scattering cross sections.

When the simplifying assumptions are dropped, it should, in principle, be possible to predict much more detailed behavior of the inelastic scattering processes, such as the dependence on nuclear well depth and shape and the nuclear wave functions.

Banerjee and Levinson have used optical-model well parameters and shell-model wave functions to analyze the elastic and inelastic scattering of protons from C^{12} at a variety of bombarding energies. They were able to predict simultaneously both the experimental behavior of the $C^{12}(p,p')$ inelastic scattering and the observed shift in the symmetry angle θ_0 for the $C^{12}(p,p'\gamma)$ angular correlation studies of Sherr and Hornyak. In so doing, they showed that the plane wave approximation to the inelastic scattering is quite poor at the energies used in the correlation studies, although at higher ($\gtrsim$150 Mev) energies the behavior of the inelastic scattering more nearly approaches that predicted by the plane wave approximation.

IV. RESULTS

In the following paragraphs, the various angles referred to are shown schematically in Fig. 1.

A. Carbon

The angular distributions for C^{12} have been reported previously[21] and the data have been extended since

[18] J. S. Blair and E. M. Henley, Bull. Am. Phys. Soc. Ser. II, **1**, 20 (1956); and private communication.

[19] S. Hayakawa and S. Yoshida, Proc. Phys. Soc. (London) **A68**, 656 (1955); Progr. Theoret. Phys. Japan **14**, 1 (1955).

[20] A. Bohr and B. Mottelson, Kgl. Danske Videnskab. Selskab, Mat.-fys. Medd. **27**, No. 16 (1953). Alder, Bohr, Huus, Mottelson, and Winther, Revs. Modern Phys. **28**, 432 (1956).

[21] Progress Report, Cyclotron Research, University of Washington, 1957 (unpublished).

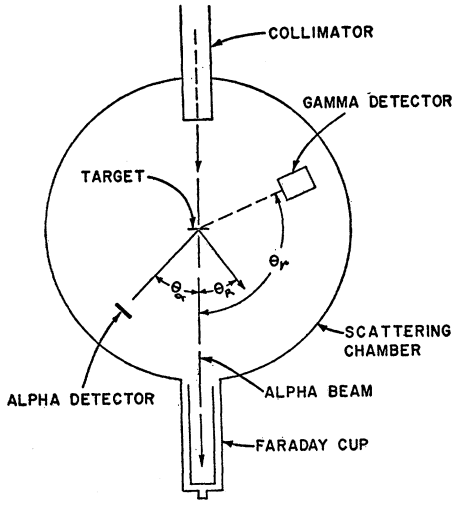

FIG. 1. Schematic drawing of scattering chamber, showing relationship of detectors to target and beam line. All angles are considered as being measured counter clockwise from the beam direction.

then.[22] The oscillatory behavior of the angular distribution of α's from the 4.43-Mev level are well represented by the $[j_2(\rho)]^2$ curve out to a momentum transfer value[23] of 2.2 f^{-1}. Using 2.21 f for the alpha-particle radius[24] gives $r_0=1.41$ f.

The angular correlation of the inelastically scattered α's (59° lab) with the gammas from the de-excitation of the 4.43-Mev level is shown in Fig. 2(a). A least-squares solution of the form $W(\theta)=C_0+C_1\sin2\theta+C_2\cos2\theta+C_3\sin4\theta+C_4\cos4\theta$ to the data points is given by the dashed line[25]; the solid line is the curve predicted on the basis of the simple assumptions ($\theta_0=\theta_R$), corrected for the finite acceptance angle of the detectors. Both curves have been arbitrarily normalized to a peak value of 1. The least-squares derived equation was used to find the minimum in the region near the recoil direction $\theta_R(=49°$ lab), which turns out to occur at $8.3°+\theta_R$ (measured counterclockwise from the beam direction). This checks well with the value, chosen by inspection, of $7.5°+\theta_R$.

A second angular correlation at an alpha scattering angle of 28°, giving $\theta_R=65°$ lab, is presented in Fig. 2(b). Here, a value of $(\theta_0-\theta_R)$ of 4° is found by inspection of the curve.

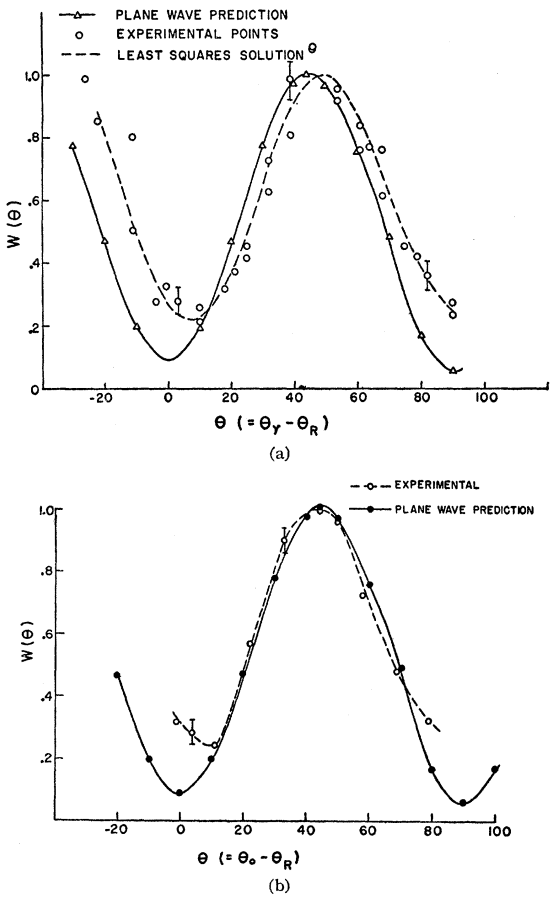

FIG. 2. (a) Alpha-gamma angular correlation for 4.43-Mev state of C^{12} in reaction $C^{12}(\alpha,\alpha'\gamma)$, for recoil angle $\theta_R=49°$. $520W(\theta)$ = coincidences per 10^5 excitations of the 4.43-Mev level. The value 8.3° for $\theta_0-\theta_R$, the difference between the observed correlation symmetry axis and the recoil direction, is obtained from the least-squares fit to the data (see text). (b) Alpha-gamma angular correlation for 4.43-Mev state of C^{12} in reaction $C^{12}(\alpha,\alpha'\gamma)$, for a value of $\theta_R=65°$. $514W(\theta)$ = coincidences per 10^5 excitations of the 4.43-Mev level. The value of 4° for $\theta_0-\theta_R$ is obtained by inspection, with a relatively large error of perhaps ±6° due to the scarcity of experimental values in the region $\theta\leq0°$. *Note.*—The abscissa in (b) should read $\theta(=\theta_\gamma-\theta_R)$.

B. Magnesium

The angular distribution of alphas from the elastic and first excited state ($Q=-1.37$ Mev) of Mg^{24} were reported by Gugelot and Rickey[4] at 43-Mev incident energy, by Watters[3] at 31.5-Mev incident energy (who also included data on the 4.2-Mev doublet), and by Vaughn[5] at 48 Mev. The data are extended in the present work to 140° (center of mass) and include the doublet state at 4.2 Mev and the state at 6.3 Mev.

Figure 3 is a plot of these distributions in the lab angle system, with arbitrary normalization of the differential cross section. The relative differential cross section values shown for the various states are as found experimentally. Figure 4 is a comparison of the elastic angular distribution with the Born approximation result for a square well potential, $[\rho^{-1}j_1(\rho)]^2$.

[22] S. F. Eccles (private communication) and A. Yavin, reference 14.

[23] The abbreviation f (=fermi) is used for 10^{-13} cm. Momentum values are quoted in units of f^{-1}.

[24] This radius is based on the interpretation of the quantity b in the equation $R=r_0A^{\frac{1}{3}}+b$ used in the article by Kerlee, Blair, and Farwell, Phys. Rev. **107**, 1343 (1957), as that describing the radius of the alpha particle, with extrapolation of the results reported in this reference to small values of A.

[25] The $W(\theta)$ given here is simply the expansion of the theoretically predicted correlation $W(\theta)=a_0+a_2\cos^2(\theta-\delta)+a_4\cos^4(\theta-\delta)$, where $\delta=\theta_0-\theta_R$.

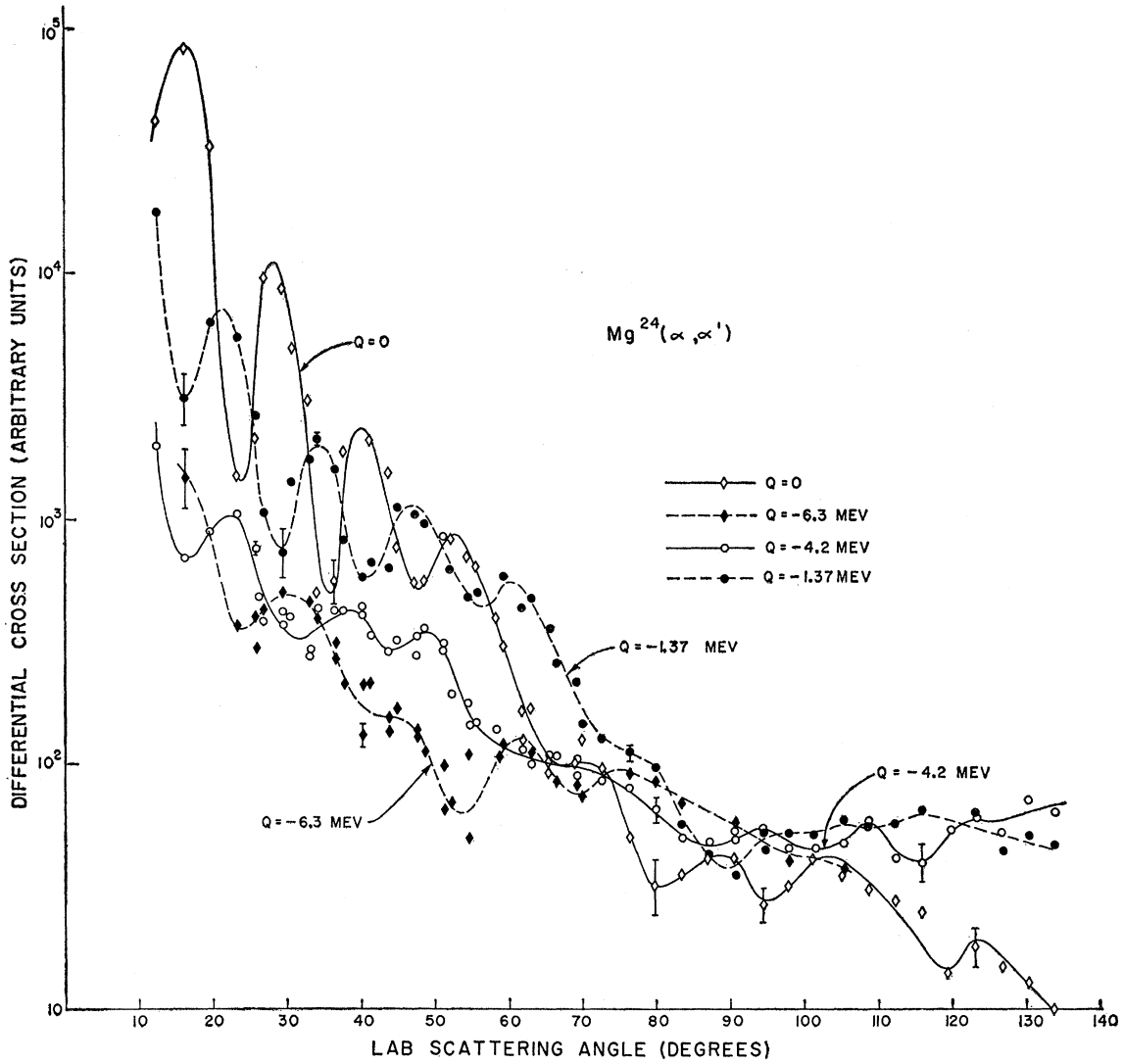

FIG. 3. Angular distribution of alpha particles from Mg^{24}, with incident laboratory energy of 43 Mev. The distributions for the ground state and first four excited states are given, with the unresolved doublet at $Q=-4.2$ Mev shown as a single curve.

From this comparison, a best fit was found at an effective radius of 6.4 f. Again, taking 2.21 f for the alpha particle radius, this gives a value of $r_0=(1.46 \pm 0.07)$ f.

Figure 5 is a comparison of the $Q=-1.37$-Mev data with the function $[j_2(\rho)]^2$ predicted by the plane wave simplification of the ABM theory for this level having known spin and parity of 2+. An effective radius for this interaction of 6.55 f is obtained, giving $r_0=(1.51 \pm 0.07)$ f. It is to be noted that the observed magnitude decreases with increasing momentum transfer faster than predicted by the theoretical curve out to about 3.5 f^{-1}, then reverses this trend and actually rises slightly beyond this value of momentum transfer ($\sim 100°$ center-of-mass scattering angle).

Figure 6 compares the data for the doublet ($Q=-4.122$, -4.24 Mev) with the theoretical functions $[j_2(\rho)]^2$ and $[j_4(\rho)]^2$. Good fits are found with both these functions, with effective radii of 6.5 f and 6.2 f, respectively. However, the data are suggestive of some combination of these two functions, for example, $[j_2(\rho)]^2+[j_4(\rho)]^2$ as given by the dashed line in Fig. 6, and indicate that both levels of the doublet may have been excited. Since the 4.122-Mev level has been found to have spin and parity 4+ and the 4.24-Mev level has been found to have spin and parity 2+, there is no *a priori* reason why both levels should not appear at our bombarding energy of 43 Mev, although Watters[3] concludes that at 31.5 Mev, only the 2+ level is excited.

The angular distribution data also included several higher energy states. A level at 5.3 Mev was observed, but was not resolvable at a sufficient number of angles to obtain a meaningful distribution. At an excitation

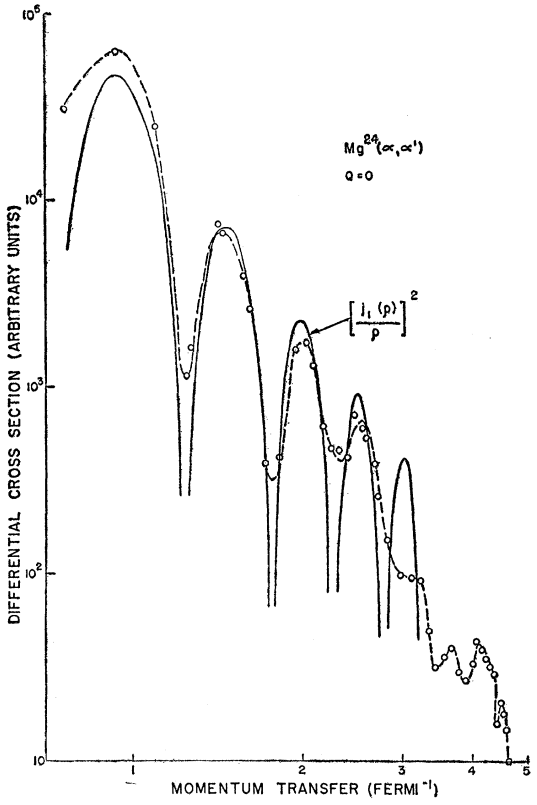

FIG. 4. Elastic scattering of 43-Mev alpha particles by Mg^{24}. The term $[\rho^{-1}j_1(\rho)]^2$ is the Born approximation result for a square well potential. The best fit of the theoretical curve to the data gives an interaction radius of 6.4 fermi.

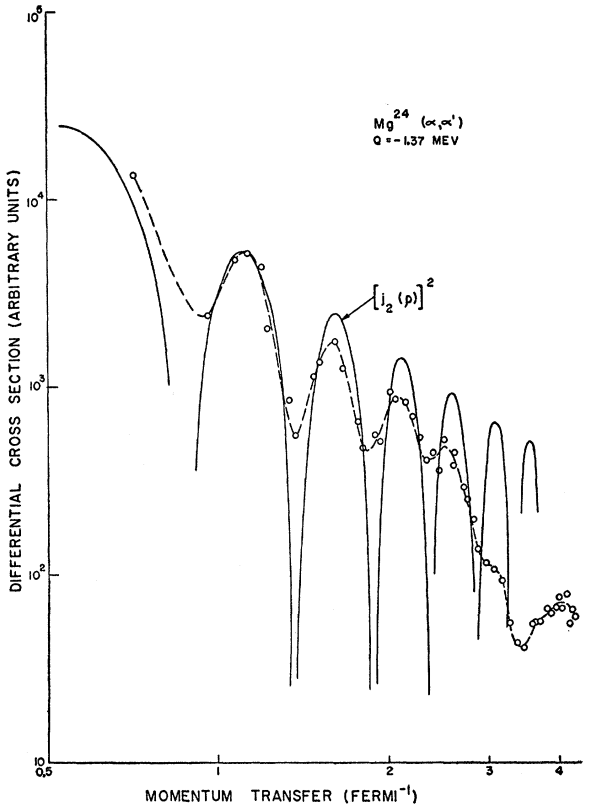

FIG. 5. Inelastic scattering of alpha particles of 43-Mev incident energy from the 1.37-Mev level of Mg^{24}. The $j_2(\rho)$ term is the second order spherical Bessel function predicted on the basis of the direct interaction process for this level.

energy of $Q=-6.3$ Mev, a level was clearly resolved for most of the angular range covered. Figure 7 shows the latter data compared with the theoretical functions $[j_1(\rho)]^2$ and $[j_3(\rho)]^2$, leading to r_0 values of 1.48 f and 1.35 f, respectively. Consistency with the effective radii found from the lower excited levels and the elastic scattering suggests assignment of spin and parity 1− to this level; however, as pointed out by Blair and Henley,[18] the fit to a $[j_1(\rho)]^2$ function may under certain conditions lead to an assignment of 0+. An angular correlation would aid in resolving this assignment. No reasonable effective radius could be found with even-value spherical Bessel function curves.

Some doubt has existed[26] as to the assignment of the 6.3-Mev level to Mg^{24} or Mg^{26}. Since the present data covered a fairly wide range of angles, the relative shift in energy with angle should be an indication as to the isotopic assignment of this level. Three curves are shown in Fig. 8 comparing the energy shift with respect to angle for 6-Mev excitation of Mg^{24}, Mg^{25} and Mg^{26}, in addition to the data obtained. The dashed line is for an excitation of 6.3 Mev in Mg^{24}. These comparisons enable one to conclude that the observed 6.3-Mev level probably belongs to Mg^{24}; the assignment of this level to Mg^{25} is not ruled out, but an assignment to Mg^{26} seems unlikely.

The angular correlation results for the 1.37-Mev level are shown in Fig. 9. The dashed line indicates the least-squares fit to the data, again by the use of the form $W(\theta)=C_0+C_1\sin2\theta+C_2\cos2\theta+C_3\sin4\theta+C_4\cos4\theta$, the solid line gives the plane wave prediction, corrected for finite acceptance angle of the detectors. The minimum in the vicinity of θ_R was found from the least-squares derived equation to be at $\theta_R+5°$. Again, this is consistent with the shift observed by inspection.

C. Calcium

The doubly magic $_{20}Ca^{40}$ nucleus was chosen as the third nucleus to be investigated for two reasons. First, it is the heaviest nucleus which can be thought of as consisting of alpha particles only, and it was hoped the results of the investigation might provide data helpful to those concerned with the alpha-particle model of the light nuclei. Second, because of the doubly magic character of the nucleus, some unusual features might

[26] See comments of P. M. Endt and J. C. Kluyver [Revs. Modern Phys. **26**, 95 (1954)] on $Mg^{24}(p,p')Mg^{24}$ data. Again, P. M. Endt and C. M. Braams, Revs. Modern Phys. **29**, 683 (1957), list this level as doubtful.

be expected. In the latter respect, the results were not disappointing. The levels reported at 3.35, 3.73, and 3.90 Mev did not show up anywhere in the angular range covered (20°–80° lab). This result was surprising when compared with the proton bombardment results at 11-Mev incident energy, where these levels showed relatively large scattering magnitude. It is suggested that these may be single-particle, rather than collective states, although it is difficult to understand why the 0+ level at 3.35 Mev did not appear in the alpha

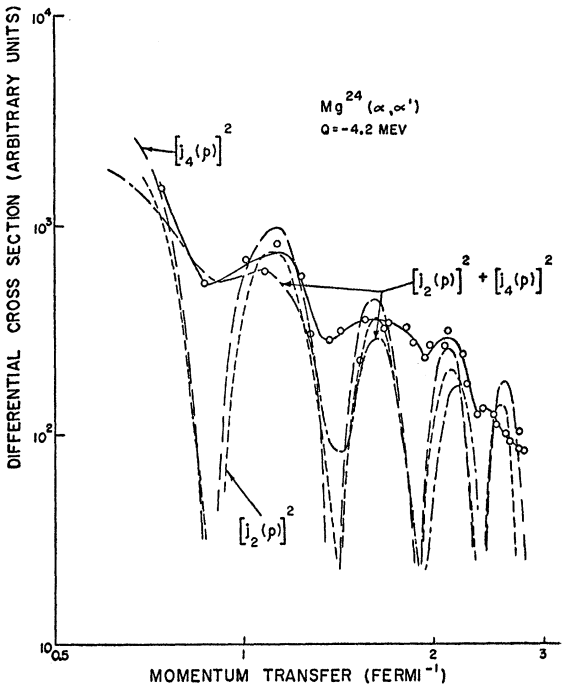

FIG. 6. Inelastic scattering of alpha particles of 43-Mev incident energy from the 4.2-Mev doublet level of Mg^{24}. The distribution is compared to the second order spherical Bessel function term (– – –) with a best fit at an interaction radius of 6.5 f, to the fourth order spherical Bessel function term (— — —) with a best fit at an interaction radius of 6.2 f, and to the sum of second and fourth order function terms (— - — -) assuming an interaction radius of 6.4 f. A comparison of the experimental distribution with those of Fig. 5 and Fig. 7 suggests that the distribution of Fig. 6 may be the sum of contributions from both 4.122-Mev and 4.24-Mev levels (unresolved) giving rise to less sharp peaks and valleys in the summed distribution than in the cases illustrated in Figs. 5 and 7.

particle bombardment, while a 0+ level at 7.6 Mev in C^{12} appears under these conditions with easily discernible amplitude over a wide range of angles.[21] The identification of the 4.48-Mev level as an odd-spin level (see below) leaves only the level at 3.90 Mev as a possible 2+ level among the first four excited states, in sharp contrast with nearly all other even-even nuclei where the first excited level is usually 2+ and low-lying. It may be significant that O^{16}, another even-even doubly magic nucleus, has a very similar level structure to Ca^{40} in the first four excited states if one is willing

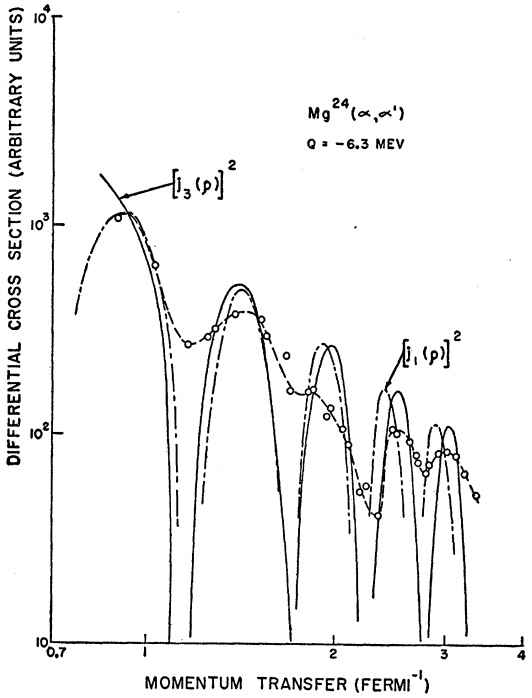

FIG. 7. Inelastic scattering of alpha particles of 43-Mev incident energy from the 6.3-Mev level of Mg^{24} (see Fig. 8 and discussion in text). The distribution is compared to the first order spherical Bessel function term (— - —) and the third order spherical Bessel function term (———), giving interaction radii 6.5 f and 6.1 f, respectively.

to guess the 3.90-Mev level in Ca^{40} as being 2+ (although, if it is 2+, its failure to appear in the present work is puzzling) and to accept the 4.48-Mev Ca^{40} level as being 1−. Again, the doubly magic Pb^{208} has a first excited level with spin and parity 3−.

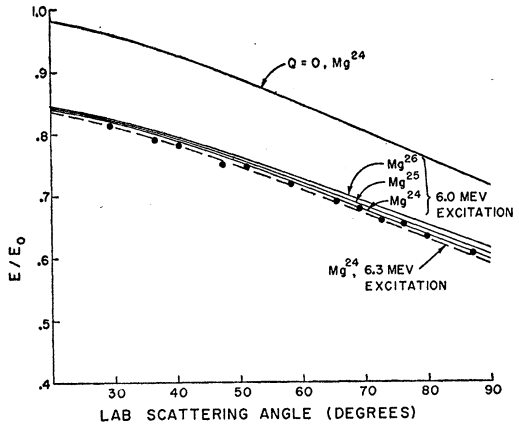

FIG. 8. A comparison of the calculated rate of change of energy *versus* scattering angle for the 6.3-Mev level in Mg^{24} with observed values. The curves of E/E_0 *versus* angle for Mg^{24}, Mg^{25}, and Mg^{26} for an excitation of 6 Mev furnish a guide for the isotopic mass assignment of the 6.3-Mev level. On this basis, the assignment to Mg^{24} is considered most likely. The dots indicating the experimental observations exceed in diameter the probable error ±0.1 Mev) of the observed values.

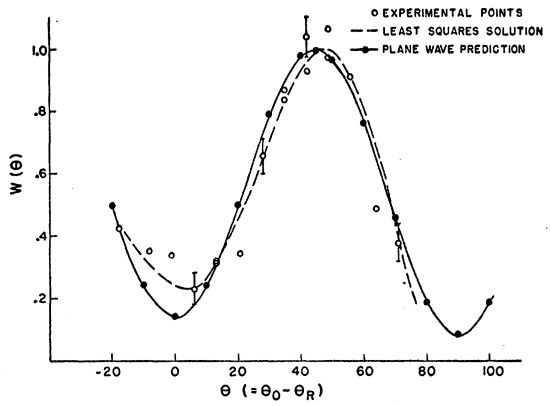

FIG. 9. Alpha-gamma angular correlation for the 1.37-Mev state of Mg^{24} in the reaction $Mg^{24}(\alpha,\alpha'\gamma)$ for a recoil angle $\theta_R=68°$. $391W(\theta)$ = coincidences per 10^6 excitations of the 1.37-Mev level. The value of 5° for the difference between the observed correlation symmetry axis θ_0 and the recoil direction θ_R is obtained from the least-squares fit to the data. *Note.*—The abscissa should read $\theta(=\theta_p-\theta_R)$.

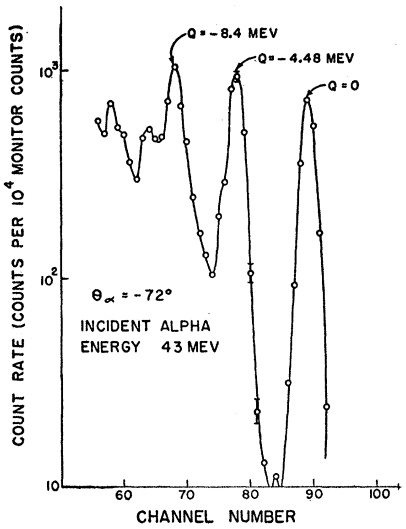

FIG. 11. Typical pulse-height spectrum ($\theta_\alpha=-72°$ lab) for alphas from the reaction $Ca^{40}(\alpha,\alpha')$. The incident alpha energy is 43 Mev.

In Fig. 10 is shown the elastic and 4.48-Mev level alpha scattering cross section with respect to scattering angle. Figures 11 and 12 show typical pulse-height spectra of scattered alphas and protons, respectively. It should be noted that in the proton spectra, the strong group at $Q=-3.7$ Mev could be the sum of contributions from the 3.73- and 3.90-Mev levels, since the resolution is not sufficient to separate the two levels. All Q values in both Figs. 11 and 12 are obtained by calibration with the well-known level separations in C^{12}, obtained under identical conditions on the same series of runs.

The comparison of the elastic alpha scattering from Ca^{40} with the Born approximation result $[\rho^{-1}j_1(\rho)]^2$

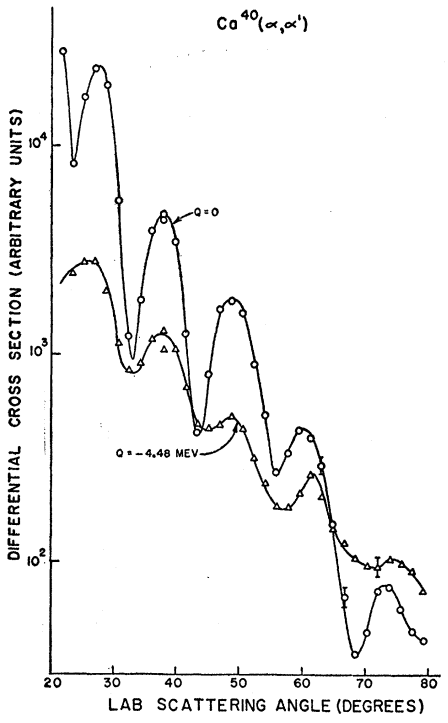

FIG. 10. Angular distribution of alpha particles scattered from Ca^{40}, with incident laboratory energy of 43 Mev. The distributions for the ground state and the 4.48-Mev level are shown.

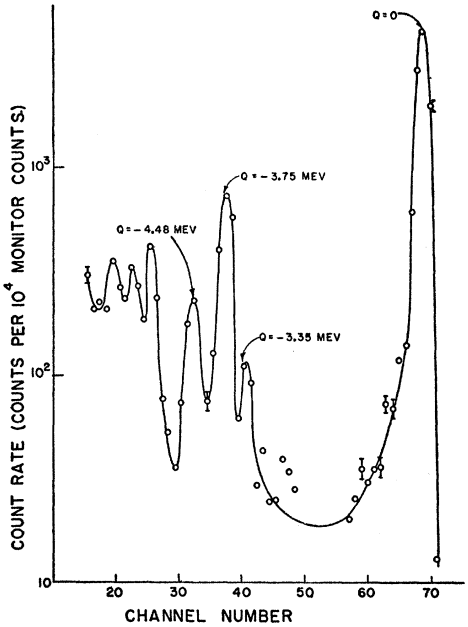

FIG. 12. Typical pulse-height spectrum of protons of incident energy 11 Mev scattered from Ca^{40}. The scattered points between the elastic and 3.35-Mev groups are due principally to oxygen and carbon impurities present in the target. The group at $Q=-3.75$ Mev (value from calibration with carbon spectrum) could be due to levels at both 3.73 and 3.90 Mev in Ca^{40}, but the shape of the curve (no broadening apparent) implies that the 3.90-Mev level is not contributing appreciably.

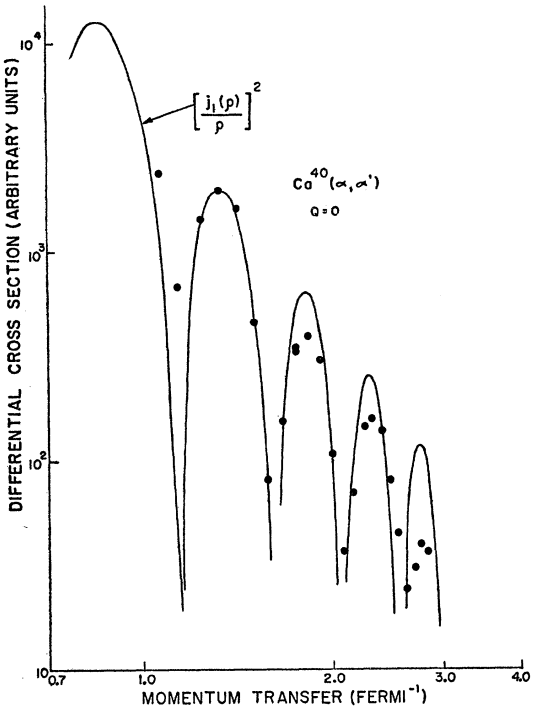

FIG. 13. Elastic scattering of 43-Mev alpha particles by Ca^{40}. Experimental results are compared to the function $[\rho^{-1}j_1(\rho)]^2$. The best fit of this Born approximation result for a square well potential to the data gives an interaction radius of 6.65 f.

shown in Fig. 13 gives an effective interaction radius of 6.65 f. Again using the value 2.21 f for the alpha-particle radius, a value of $r_0=(1.30\pm0.06)$ f is obtained.

This value of r_0 is significantly smaller than those found from the C^{12} and Mg^{24} data, and probably represents the effect of the doubly closed shell character of this nucleus. The effective interaction radius of 6.65 f should be compared also with the value 7.12 f found[6] for A^{40}. No such reduction in radius is to be expected on the basis of any model except the shell model.

A comparison of the data for alpha scattering from the 4.48-Mev state with the function $[j_3(\rho)]^2$ is given in Fig. 14. The lack of information at smaller momentum transfer values is unfortunate, since with the available data, a fit almost equally good is found with the $[j_1(\rho)]^2$ curve. The radii from these two comparisons are $r_0=(1.39\pm0.06)$ f and $r_0=(1.49\pm0.06)$ f, respectively. The comparison with even-value spherical Bessel functions all gave quite unreasonable values to r_0, as well as providing poorer fits to the various maxima and minima. Thus, one can conclude from these data only that the 4.48-Mev level is probably either 1− or 3−, with a slight preference for the 3− assignment based on the fact that the r_0 value for this spin and parity is more consistent with that found from the elastic scattering.

It should be noted in the graph of the alpha spectrum, Fig. 11, that levels higher than the 4.48-Mev level appear. Of these, only the one appearing at 8.4 Mev showed up with enough consistency and resolution from surrounding levels to permit an identification. Figure 15 shows the ratio E/E_0 at which this level appeared *versus* scattering angle, compared to the E/E_0 ratio for the elastic and 4.48-Mev groups. Again using the calibration afforded by the C^{12} level separation and a knowledge of the target thickness, the Q value of this level is found to be (8.4 ± 0.2) Mev. This value lies in an intermediate energy region where other investigators[27,28] have not reported levels.

No attempt is made to assign spin and parity to this new level, since an insufficient angular range, especially over small angles, was covered and the scattering cross section at many angles was difficult to obtain with accuracy.

A series of attempts was made to obtain an angular correlation of the 4.48-Mev level alpha scattering with gamma rays of energy greater than 2.0 Mev. The results were not consistent with a direct transition to the ground state and seemed at first to indicate that the scattering process might be taking place via some compound nucleus mechanism, although the angular distribution data were consistent with the direct-interaction scattering theory. It was decided then to investigate the mode of decay of this state by means of coincidence analysis of inelastic proton scattering groups and any

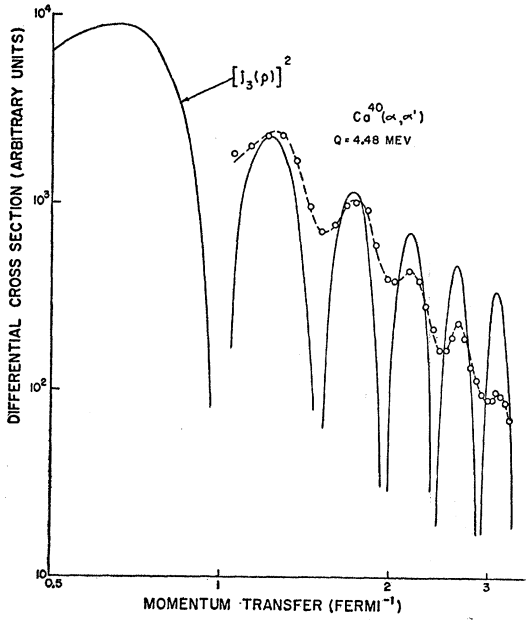

FIG. 14. Inelastic scattering of 43-Mev incident energy alpha particles from the 4.48-Mev state of Ca^{40}. The $[j_3(\rho)]^2$ term is the third order spherical Bessel function term predicted on the basis of direct interaction theory with the assignment of 3− spin and parity for this level. The best fit of this function to the data gives an interaction radius of 7.3 f. A similar comparison with the function $[j_1(\rho)]^2$ (not shown) gives an interaction radius of 7.0 f.

[27] Towle, Berenbaum, and Mathews, Proc. Phys. Soc. (London) **A70**, 84 (1957).
[28] C. M. Braams, Phys. Rev. **101**, 1764 (1956).

resultant gamma rays. The pulse-height spectra of gammas gated with the 4.48-Mev and 3.7-Mev group protons scattered by Ca^{40} were obtained and compared with the gamma spectrum obtained by gating with the 4.43-Mev group protons scattered by C^{12}. If the 4.48-Mev level in Ca^{40} were decaying directly to the ground state, the gated spectrum should be nearly identical with that for the gated C^{12} spectrum. This was not the case; rather there resulted a nearly identical gated gamma spectrum for the two Ca^{40} levels, indicating that the 4.48-Mev level of Ca^{40} is decaying principally by cascade through the 3.7-Mev level to ground. It was not possible to determine with certainty whether the intermediate state is the 3.73- or the 3.90-Mev state, because of an inability to discriminate between these two proton groups.

An analysis of the angular correlation in view of this result is complicated. It constitutes a triple correlation with intermediate gamma unobserved, a situation analyzed in the literature.[17,29] In view of the uncertainty as to the assignment of spin and parity for the 4.48-Mev level and the spin of the intermediate state, several cascade possibilities exist. These have been investigated on the assumption that only pure transitions are involved. The only possibility which even qualitatively fits the observed correlation (Fig. 16) is that the 4.48-Mev state is 1−, with cascade through either 2+ or 3− level. Figure 17 shows the level scheme for Ca^{40} postulated on the basis of information from reference 26 and the present work.

The correlation function for this latter case is still simple and depends on the knowledge of the j value of each level in the cascade and the multipolarity of the transitions between levels. With the assumption that the 4.48-Mev level is (1−), $j_2=3-$, and unobserved

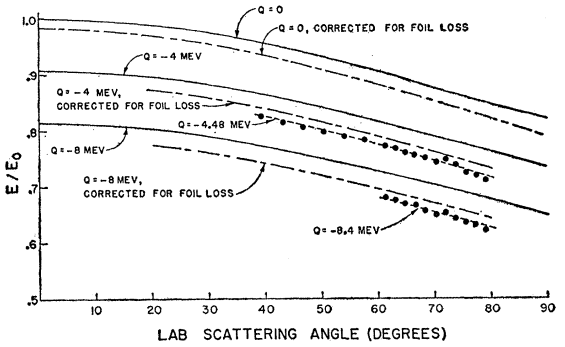

FIG. 15. A comparison of the rates of change of energy *versus* scattering angle observed for the 4.48-Mev and 8.4-Mev levels in Ca^{40} with calculated rates of change for several excitation energies. Since the calcium foil used was relatively thick (16 mg/cm) corrections were necessary for the average alpha particle energy loss in the foil. The corrected values of E/E_0 are shown as the first dashed (— - —) curves below the solid curves for $Q=0$, -4, and -8 Mev. These corrected curves were then used to establish the values 4.48 Mev and 8.4 Mev for the excitations observed.

[29] Biedenharn, Arfken, and Rose, Phys. Rev. **83**, 586 (1951).

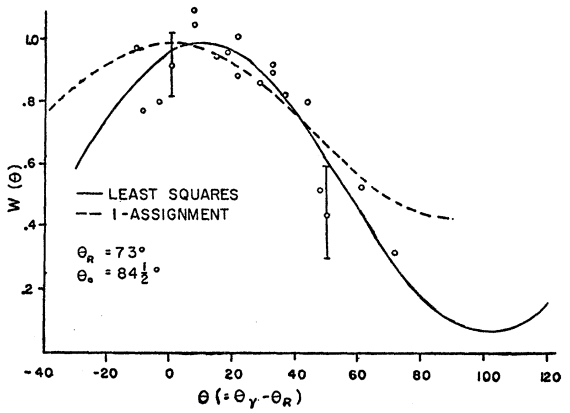

FIG. 16. Alpha-gamma angular correlation for 4.48-Mev state of Ca^{40} in reaction $Ca^{40}(\alpha,\alpha'\gamma_1)Ca^{40*}(\gamma_2)Ca^{40}$ for a value of $\theta_R=73°$. $500W(\theta)$ = coincidences per 10^5 excitations of 4.48-Mev level. The curve for the angular correlation predicted on the basis of spin and parity assignment of 1− for the 4.48-Mev level, 3− for the intermediate level and quadrupole unobserved radiation is shown by the dashed line. The solid line is the least-squares curve assuming the 4.48-Mev level is 1−. A θ_0 value of $11\frac{1}{2}°+\theta_R$ is obtained from the least-squares analysis.

radiation is quadrupole, one gets the simple correlation form $W(\theta)=1+\frac{3}{5}P_2(\cos\theta)$.

In the graph of this correlation, Fig. 16, the dashed line represents the prediction for the 1− assignment to the 4.48-Mev level. Thus, the experimentally observed angular correlation can be said to furnish supplementary evidence for the assignment of spin and parity 1− to the level at 4.48 Mev.

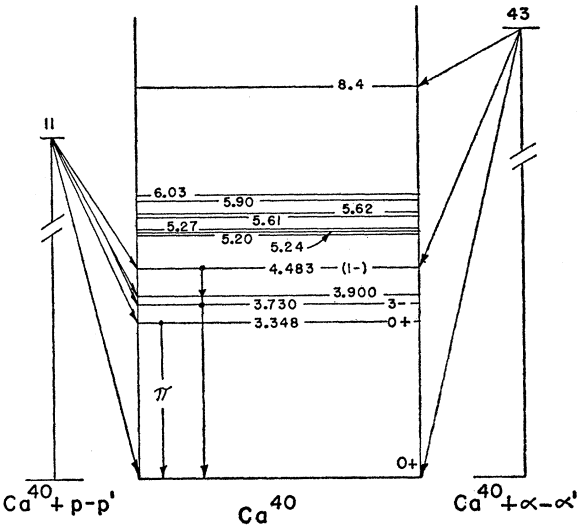

FIG. 17. Energy level diagram of Ca^{40}. Levels shown are obtained from present work and reference 26. The reactions $Ca^{40}+p-p'$ and $Ca^{40}+\alpha-\alpha'$ diagrammed at either side of the energy level diagram represent the present work only. The doublet level at 3.73 and 3.90 Mev with arrows from the $Ca^{40}+p-p'$ reaction was not resolved in the present work. Energies of the various levels shown are in Mev. The spin and parity assignment of the 4.48-Mev level and the energy value for the 8.4-Mev level are from the present work, as is the gamma cascade indicated from the 4.48-Mev level.

V. DISCUSSION

A. Target Impurities

Impurities existed in all three targets.

1. Carbon

In the carbon target, oxygen and nitrogen were present in small amounts. Both were easily identified and gave no trouble.

2. Magnesium

The magnesium target was of natural isotopic materials (Mg^{24}—78.8%, Mg^{25}—10.1%, Mg^{26}—11.1%). Many levels previously reported above the 4.24-Mev level in Mg^{24} are now suspect as belonging to one or another of the heavier isotopes.[26] Figure 8 is presented as evidence that the 6.3-Mev level should be assigned to Mg^{24}, although it is conceded that the evidence is not conclusive. It is difficult to imagine, however, that the 6.3-Mev level scattering magnitudes shown relative to the elastic and 1.37-Mev groups in Fig. 6 could arise from either heavier isotope of ~10% abundance.

3. Calcium

The Ca^{40} target showed some oxygen contamination and a trace of carbon. At laboratory scattering angles less than 25°, these presented some difficulty, especially in defining the 4.48-Mev group. At larger angles, the large disparity in masses was helpful in removing these impurities from the region of interest as the scattering angle increased.

B. Finite-Geometry Correction

The correction of the theoretically predicted angular correlation for the effects of finite geometry requires knowing (a) the form of the correlation, (b) the gamma-ray absorption coefficient to be used. In the case of C^{12} and Mg^{24} correlations, the expected correlation form on the basis of pure transitions and direct interactions using the plane wave assumptions is, for point detectors,

$$W(\theta)=1+0.714P_2(\cos\theta)-1.714P_4(\cos\theta),$$

where θ is the angle between scattered alpha and coincident gamma, or alternatively, the target nucleus classical recoil direction and coincident gamma. (See following paragraph.) In the Ca^{40} correlation, no attempt was made to correct for finite geometry. The pertinent gamma ray absorption coefficients were obtained from a tabulation by Miller, Reynolds, and Snow.[30]

The finite-geometry correction made here and that outlined by Rose[31] differ slightly. The situation analyzed by Rose is in terms of the angle between alpha-counter and gamma-counter center lines, while in this work the angle $\theta=\theta_R-\theta_\gamma$ is used. That the finite geometry corrections are not entirely equivalent is easy to demonstrate, since the relationship between the solid angle of the alpha-crystal and the resultant solid angle of the recoil directions is dependent on "external parameters" such as energy, Q value of the nuclear reaction, recoil mass, and scattering angle.

However, for all correlations in the present work, the alpha-scattering angle was sufficiently large so that the ratio $\Delta\Omega$(recoil)/$\Delta\Omega$(alpha crystal) was always less than one. (This would not be true at very small alpha-scattering angles.) Therefore, in view of the very small $\Delta\Omega$ defined by the half-angle subtended of less than 1° for the alpha crystal, the assumption was made that detection of an alpha particle at θ_α was entirely equivalent to detection by a point detector of the recoil nucleus at θ_R. The solid angle of the gamma detector was characterized by the half-angle subtended of 21° 20′.

Effects due to recoil of the emitted gamma radiation on the direction of recoil of the target nucleus were ignored, since in the extreme case considered, this resulted in an angular deviation of less than 1° from the original recoil direction.

C. Results

Table I presents in tabular form the various Q values and effective interaction radii for the nuclear levels investigated, together with their spin and parity assignments as deduced from this work and as reported in the survey reviews on energy levels in light nuclei.[26,32] Also listed are the available data on $(\theta_0-\theta_R)$.

Various direct interaction theories[2,18,19] all have in common (in the plane wave approximation) the prediction that the angular distributions should be represented in terms of appropriate spherical Bessel functions. The data in references 13, 14, and the present

TABLE I. Summary of level information and angular correlation results. All reactions are (α,α') with incident alpha energy of 43 Mev.

Target	Q for reaction (Mev)	Effective interaction radius (10^{-13} cm) from present work	Spin and parity	$\theta_0-\theta_R$ (lab deg)
C^{12}	−4.43		2+	57–49[a] 69–65[a]
Mg^{24}	0	6.4	0+	
	−1.37	6.55	2+	73–68[a]
	−4.2	6.5 (6.2)	2+ (4+)[a]	
	−6.3[a]	6.5	1− (0+)[a]	
Ca^{40}	0	6.65	0+	
	−4.48	7.3	1−[a]	84–73[a]
	−8.4[a]			

[a] Values from present work.

[30] Miller, Reynolds, and Snow, Rev. Sci. Instr. **28**, 717 (1957).
[31] M. E. Rose, Phys. Rev. **91**, 610 (1953).
[32] F. Ajzenburg and T. Lauritsen, Revs. Modern Phys. **27**, 77 (1955).

work strongly support this feature, while at the same time indicating just as clearly that the Bessel functions are no better than a good first approximation. This is made clear by inspection of the various comparisons of angular distributions with the spherical Bessel functions presented in references 13, 14, and the present work. Two features frequently encountered are the failure of the $[j_l(\rho)]^2$ to represent the correct rate of change of differential cross section with scattering angle (alternatively, with momentum transfer) and the failure to represent correctly the various maxima and minima at large values of momentum transfer. The differences in the predictions of the theories mentioned above as far as angular distributions are concerned (again in the plane wave approximation) lie principally in the magnitudes of the cross sections. Since no attempt was made in the present work to obtain absolute values for the scattering amplitudes, no magnitude comparisons can be made.

It should be pointed out that while the spherical Bessel function as an approximation to the dependence of the scattering with respect to angle seems quite valid for alpha particle scattering at 43 Mev, the work of Sherr and Hornyak[12,16] clearly indicates that the same approximation functions completely fail to predict proton scattering angular distributions from light nuclei at bombarding energies less than 20 Mev. On the other hand, the values of $(\theta_0-\theta_R)$ from the present work are the same magnitude as those found by Sherr and Hornyak for comparable values of momentum transfer. It would appear that the quantization axis θ_0 of the excited recoil nuclei which subsequently decay to the ground state by gamma emission is never very different from the classical recoil direction θ_R (except for momentum transfer values less than 1 f^{-1}), arguing for the approximate validity of the plane wave approximation, but that strong scattering amplitude corrections dependent on momentum transfer are needed to interpret the angular distributions successfully over a range of bombarding energies. If one assumes a direct interaction between incident alpha particles and alpha-particle-like groups of nucleons in the target nucleus[18] or if the interaction is assumed to take place with collective modes of motion of the target nucleus,[19] one would expect a much more gradual drop-off of cross section with angle than in the interaction with single nucleons in the target nucleus, an effect which can be used at times to distinguish single-particle levels. In either case, detailed analysis is needed to justify any more than qualitative statements regarding the scattering amplitude corrections.

VI. SUMMARY

The proposal that inelastic scattering of nuclear particles from nuclei proceeds principally by direct interaction rather than some variation of compound nucleus interaction seems well validated as far as the conditions of the present work are concerned. The trend toward larger scattering cross sections at large values of momentum transfer (not predicted by ABM) noted here, and in references 5, 13, 14, and 21, would indicate that the interaction occurs with some collective mode of the target nuclei rather than with single nucleons in the target nucleus.

As noted above, the plane wave approximation seems sufficiently good to predict the general behavior of inelastic scattering of alphas in the energy range 30 to 48 Mev and of alpha-gamma angular correlations, but it fails when applied to the finer features of both the inelastic scattering and the angular correlations. This failure is not surprising in view of the rather unrealistic nature of the approximation; what is more interesting is that the plane wave approximation is as good as it appears to be. Thus, one is forced to conclude that direct interactions under the experimental conditions typical of the present work (light nuclei, 30–40 Mev alpha energy) proceed mainly by interaction very close to the nuclear surface involving some collective mode of motion of the target nucleus, and that distortion of the wave function of the bombarding particle is evident, but is apparently not severe.

ACKNOWLEDGMENTS

The author wishes to express his appreciation of the support and encouragement of Professor G. W. Farwell, valuable discussions with Professor J. S. Blair and Professor E. M. Henley, and the considerable assistance of the University of Washington Cyclotron crew. Special thanks are due to Dr. P. C. Robison who collaborated in the early stages of the work and was generally helpful throughout the investigation.